

Published in final edited form as:

NMR Biomed. 2013 December ; 26(12): . doi:10.1002/nbm.3014.

Diffusion-Weighted MRI Monitoring of Pancreatic Cancer Response to Radiofrequency Heat-Enhanced Intratumor Chemotherapy

Tong Zhang, MD, PhD^{1,2,†}, Feng Zhang, MD, PhD^{1,†}, Yanfeng Meng, MD, PhD¹, Han Wang, MD, PhD¹, Thomas Le, MD¹, Baojie Wei, MD, PhD¹, Donghoon Lee, PhD¹, Patrick Willis¹, Baozhong Shen, MD, PhD^{2,*}, and Xiaoming Yang, MD, PhD^{1,*}

¹Image-Guided Bio-Molecular Intervention Research and Section of Vascular & Interventional Radiology, Department of Radiology; University of Washington School of Medicine, Seattle, WA, 98109

²Department of Radiology, Haerbin Medical University Affiliated 4th Hospital, Haerbin, China 150001

Abstract

PURPOSE—To evaluate the feasibility of using diffusion-weighted MRI to monitor the early response of pancreatic cancers to radiofrequency heat (RFH)-enhanced chemotherapy.

MATERIALS AND METHODS—Human pancreatic carcinoma cells (PANC-1) in different groups and twenty four mice with pancreatic cancer xenografts in four groups were treated by phosphate buffered saline (PBS) as a control, RFH at 42 °C, gemcitabine and gemcitabine plus RFH at 42°C. One day before and 1, 7, and 14 days after the treatment, diffusion-weighted MR imaging and T2 weighted imaging were applied to monitor the apparent diffusion coefficients (ADCs) of tumors and tumors growth. MRI findings were correlated with results of tumors apoptosis analysis.

RESULTS—Of the in vitro experiments, quantitative viability assay showed lower relative cell viabilities treated by gemcitabine plus RFH at 42°C, compared to those by RFH only and gemcitabine only ($37\% \pm 5\%$ vs $65\% \pm 4\%$ and $58\% \pm 8\%$, $p < 0.05$). Of the in vivo experiments, the combination therapy resulted in smaller relative tumor volume than RFH-only and chemotherapy-only (0.82 ± 0.17 vs 2.23 ± 0.90 and 1.64 ± 0.44 , $p = 0.003$). In vivo 14T MRI demonstrated a remarkable decrease of ADCs at day 1 and increased ADCs at days 7 and 14 in the combination therapy group. The apoptosis index in the combination therapy group was significantly higher than those in the groups of chemotherapy-only, RFH-only and PBS treatments ($37\% \pm 6\%$ vs $20\% \pm 5\%$, $8\% \pm 2\%$, and $3\% \pm 1\%$, $p < 0.05$).

CONCLUSION—This study confirms that it is feasible to use MRI to monitor RFH-enhanced chemotherapy on pancreatic cancers, which may present new options for efficient treatment of pancreatic malignancies using MR/RF-integrated local chemotherapy.

*Correspondence to: Xiaoming Yang, MD, PhD, Image-Guided Bio-Molecular Intervention Section, Department of Radiology, University of Washington School of Medicine, 850 Republican Street, S470, Seattle, Washington, USA., Phone: 206-685-6967, Fax: 206-221-0647, xmyang@u.washington.edu.

†Contributed equally as the first authors.

*Contributed equally as corresponding authors

Introduction

In spite of enormous efforts of research in the past decade, pancreatic carcinoma is still one of the leading causes of cancer deaths in the world, and most pancreatic cancer patients died within one year after the diagnosis (1). Surgical eradication is the only curative treatment approach for pancreatic cancers. However, most patients are not candidates for surgery due to either metastasis or the presence of locally advanced disease, and thus the palliative treatment with chemotherapy has been the first choice for the majority of such patients.

Gemcitabine is currently the standard first-line chemotherapeutic drug in the treatment of advanced pancreatic cancer (2). However, clinical data shows that gemcitabine alone or gemcitabine-based combination chemotherapy is not likely to achieve the goal of tumor control due to the high intrinsic resistance of pancreatic cancers to gemcitabine (3). Therefore, it is essential to explore alternative approaches for efficiently treating pancreatic carcinomas. A recent study shows that a combination therapy of regional hyperthermia with gemcitabine and cisplatin can improve the time to progression, the overall survival and the disease control rate for patients with gemcitabine-refractory advanced pancreatic cancer (4). Protein denaturation of cancer cells is the main molecular event underlying the biological effects of hyperthermia when applying a temperature range of 39 – 45 °C (5). This phenomenon motivated us to combine hyperthermia with chemotherapy, to achieve synergistic therapeutic effect on pancreatic carcinomas. A MR imaging/radiofrequency (RF) heating system, with its key component being an FDA-approved MR-imaging-heating-guidewire (MRIHG) has previously been used to deliver external RF heat energy to enhance gene expression (6). We may use the heat generated by the MRIHG to treat pancreatic cancers.

Conventional imaging criteria for the clinical evaluation of therapeutic response in cancer are based on the Response Evaluation Criteria in Solid Tumors guidelines (RECIST). However, RECIST lacks the ability to predict the early response of cancers to treatments (7). Diffusion-weighted magnetic resonance imaging (DWI) is one of preferentially used imaging modalities in evaluating the early response of cancers to anti-cancer therapies (8–10). Preceding the change of tumor morphology and size after the therapy, DWI can demonstrate the biological and physiological changes of cancers at the cellular and molecular level (10–12). The aim of this study was to investigate the capability of using MRIHG-created RF heat to enhance chemotherapy for pancreatic cancers, which was monitored by 14T MRI.

Materials and Methods

Study Design

This study was divided into two phases: (a) *in vitro* experiments using pancreatic cancer cells to confirm RFH-enhanced chemotherapeutic efficacy on pancreatic malignancies; and (b) *in vivo* experiments on mice to validate the feasibility of using diffusion-weighted MRI to monitor the response of pancreatic cancers to RFH-enhanced chemotherapy.

In Vitro Experiments

Cell lines and cell culture

Human pancreatic cancer cells (PANC-1) (ATCC, Manassas, VA) were maintained in Dulbecco's Modified Eagle Medium (DMEM) containing 10% fetal bovine serum (Mediatech Inc., Manassas, VA). 1×10^5 cells were seeded and cultured in each chamber of the four-chamber cell culture plates (NalgeNunc International, Rochester, NY). When the cells confluence reached 80%, experiments were initiated. Cells in chambers were divided

into different groups: group 1 was treated by 50 nM gemcitabine for 24 hours plus RFH at different temperatures (38°C, 40°C and 42°C for 20 minutes); group 2 received gemcitabine only for 24 hours; group 3 received RF (38°C, 40°C and 42°C for 20 minutes); and group 4 without treatment as a control.

MRIHG-mediated RF heating

For the cell groups with MRIHG-mediated RF heating, the cell culture plate was placed in a 37 °C water bath. The hot spot of the MRIHG was attached under the central bottom of chamber 4 of the cell culture plate and then connected to the custom RF generator for heating (Figure 1 A). During heating, a 1.1-mm temperature sensing probe (Photon Control Inc, Burnaby BC, Canada) was placed under the bottom of each of the four chambers to record the temperature. Cells in chamber 4 were heated to approximately 42 °C for 20 minutes by adjusting the output power at 15 watts. After heating, cells were kept in the incubator for 24 hours.

Cell viability Assay

Cells were rinsed with phosphate-buffered saline (PBS) and trypsinized by 0.05% trypsin. The viable cells were counted by trypan blue exclusion using an automatic cell counter (TC10, Bio-Rad Laboratories Inc, CA).

In Vivo Experiments

Creation of animal models with pancreatic cancer xenografts

The animal protocol was approved by the Institutional Animal Care and Use Committee. Female nu/nu mice at 4–6 weeks age (Charles River Laboratories, Wilmington, MA) were used to create the tumor model. A suspension of 5×10^6 PANC-1 cells in 50 μ L of PBS was injected subcutaneously and unilaterally in the back of each mouse to create pancreatic cancer mass. Within 3–4 weeks, the tumor mass grew to approximately 5 mm in diameter. Tumor-bearing mice were then randomized to four groups: group 1 (6 mice) received intratumoral injection of PBS to serve as a control; group 2 (6 mice) was treated by RFH only; group 3 (6 mice) received intratumoral injection of 20 mg/kg gemcitabine; and group 4 (6 mice) was treated by intratumoral injection of gemcitabine plus RFH via the MRIHG.

RF heating

Mice were anesthetized by means of inhalation of 1%–3% isoflurane in oxygen. The hot spot of the MRIHG and a 400- μ m temperature sensor were positioned, side-by-side, into the tumor mass. By adjusting the output power according to the temperature reading on the temperature sensor, the temperature was kept at 42°C in each mass for 20 minutes.

14T MRI and imaging analysis

Anesthesia was maintained by delivery of 1.5%–2% isoflurane in oxygen throughout the entire MRI period. MR imaging was performed using 14T vertical wide bore Magnetic Resonance Spectrometer (Bruker Corporation, Billerica, MA). T2 weighted imaging (T2WI) and DWI were used to image the tumors 1 day prior and 1, 7, and 14 days after the treatment. Animals were placed in a 25-mm-diameter micro-imaging coil (Bruker Corporation, Billerica, MA) for imaging acquisition. T2 weighted images were acquired using the rapid acquisition with relaxation enhancement (RARE) sequence: repetition time (TR)/echo time (TE) = 890 msec / 4.5 msec; field of view = 2.56 cm; matrix = 128 \times 128; section thickness = 1mm; intersection gap = 0 mm; number of averages = 4; rare factor = 8; refocusing flip angle = 180°; 4 averages; fat suppression with a Gaussian pulse, pulse length = 1.6 ms and bandwidth = 1750 Hz; 10–15 slices; and a total scan time of 57 sec. Two-

dimensional (2D) spin-echo diffusion-weighted MR images were then acquired with diffusion factors (b factor) of 0, 500 and 1000 s/mm²; TR /TE = 3000 msec/27.5 msec; field of view = 25.6×25.6 mm; matrix size = 128×128; and a total scan time of 19 min and 12 sec.

For ADC measurements, the image section with the largest tumor diameter was selected for generating the ADC map and ADC was measured using ImageJ (National Institute of Health). The region of interest (ROI) for calculating ADC values was manually delineated encompassing the entire tumor using the same section of the T2W image as a reference. Tumor volume measurements and segmentation of tumors were made using ImageJ. Due to the variation of tumor sizes at the initial stage of the treatment, we used relative tumor volume (RTV) for tumor growth comparison, which is expressed as a ratio relative to tumor volume at baseline and calculated according to the following equation: $RTV = TV_n / TV_0$, where TV_n is the tumor volume at day n and TV_0 was the tumor volume at day 0 (13).

Histology

After achieving satisfactory MRI, all mice were euthanized by CO₂ respiration for 5 minutes. Each tumor mass was harvested, cryosectioned at 8- μ m slices and then stained for histopathologic examination. Apoptosis of tumor masses was evaluated by terminal deoxynucleotidyl transferase-mediated dUTP nick end labeling (TUNEL) using an in situ apoptosis detection TUNEL kit (Trevigen, Gaithersburg, MD) following the protocol provided by the manufacturer. Cells with dark blue dots in the cytoplasm were recognized as apoptotic cells. Six fields were randomly pictured using an Olympus DP72 digital camera (Olympus, Tokyo, Japan) on one slide, which accounted for approximately 500–700 cells for each tumor. Results are expressed as the apoptotic index: Apoptotic Index% (AI) = (the number of positive cells/the total number of cells in the field)×100%.

Statistical analysis

The statistical software (SPSS, version 19.0; SPSS Chicago, Ill) was used for all data analyses. All data were presented as mean \pm standard deviation. A non-parametric Mann-Whitney U test was used to compare: relative viability between cell groups; and ADCs and relative tumor volumes at different time points between mouse groups. $P < 0.05$ was considered as the significant difference.

Results

In the *in vitro* experiments, when chamber 4 was heated up to 42°C from 37°C, a temperature gradient was achieved through the four chambers: 42°C at chamber 4; 40°C at chamber 3; 38°C at chamber 2 and no temperature increase at chamber 1 (37°C) (Figure 1A). Gemcitabine plus RFH at 42°C resulted in the lowest relative cell viability in comparison to gemcitabine-only (37% \pm 5% vs 58% \pm 8, $p < 0.05$) and RFH-only (37% \pm 5% vs 65% \pm 6%, $p < 0.05$) (Figure 1B). The relative cell viability is the lowest for the cell group receiving the chemotherapy at 42°C than those at 40°C (37% \pm 5% vs 45% \pm 4%, $p < 0.05$) and at 38°C (37% \pm 5% vs 54% \pm 3%, $p < 0.05$) (Figure 1B). In addition, in the cell group with RFH-only at 42°C also demonstrated hyperthermia-induced cell killing effect in comparison to the lower temperatures of 38°C and 40°C (65% \pm 6% vs 77% \pm 4% and 65% \pm 6% vs 90% \pm 6%, $p < 0.05$) (Figure 1B).

For in-vivo experiments, all mice survived the procedures throughout the entire experiments. Figure 2 shows representative MR T2-weighted images of different study groups. The average tumor volume of tumors before treatment in the PBS group, RFH-only group, chemotherapy-only group and combination therapy group is $1.28 \pm 0.22\text{cm}^3$, $1.79 \pm 0.21\text{cm}^3$, $2.01 \pm 0.20\text{cm}^3$ and $2.07 \pm 0.11\text{cm}^3$. The relative tumor volume was smaller in the group

receiving gemcitabine plus RFH as compared to those of the animal groups receiving gemcitabine-only (0.82 ± 0.17 vs 1.64 ± 0.44 , $P < 0.05$) and RFH-only (0.82 ± 0.17 vs 2.23 ± 0.90 , $p < 0.05$) (Figure 3). Regarding ADCs at day 1, the average ADC of the chemotherapy plus RFH group remarkably decreased 1 day after the treatment, and increased 7 and 14 days after the treatment (Figure 4). The apoptosis index in group 4 was significantly higher than those in other three groups treated by gemcitabine-only ($37\% \pm 6\%$ vs $20\% \pm 5\%$, $p < 0.05$), RFH-only ($37\% \pm 6\%$ vs $8\% \pm 2\%$, $p < 0.05$) and control ($37\% \pm 6\%$ vs $3\% \pm 1\%$, $p < 0.05$), indicating the enhanced cell killing effects when combining gemcitabine with RF-heating (Figure 5).

Discussion

Pancreatic cancer is one of the most difficult malignancies to treat and has a very high mortality rate. Once diagnosed, most patients with pancreatic cancers are usually at the late stages of disease, often with metastatic spread. For the small proportion of patients at the early stage, surgical resection is an option for the treatment, but the majority of the patients suffering from pancreatic cancers have no chance to receive surgery (14). Thus, the management of pancreatic cancer is still a major medical challenge worldwide.

In the past decade, the primary chemotherapeutic drug for advanced pancreatic cancers has been the deoxycytidine analogue, gemcitabine (9). However, the outcome of gemcitabine-based chemotherapy is dismal, due to inefficient drug delivery into tumor tissues and the high resistance of cancer cells to gemcitabine (15). Thus, it is essential to explore new approaches to effectively manage this life-threatening malignancy.

Recent studies have confirmed that hyperthermia can enhance the killing efficacy of chemotherapy on cancer cells, via the potential mechanisms of increasing chemotherapeutic drug entry to cancer cells, enhancing chemotherapeutic cytotoxicity, and thereby inducing cellular death and necrosis (5). The positive results of randomized clinical trials confirmed hyperthermia combined with chemotherapy as a novel clinical approach for the treatment of cancers (16–19). Some studies have demonstrated that the thermal enhancement of cytotoxicity of chemotherapeutic agents can be reached at hyperthermia temperatures between 40.5°C and 43.0°C (20, 21).

For the generation of hyperthermia in the body, it is critical to create localized heat at the target tumor mass only, and avoid injuring the surrounding organs and tissues. In this study, we specifically used MR-imaging-heating-guidewire (MRIHG) to deliver external RF energy into the targeted tumor area only. The 0.022-inch MRIHG is made of a coaxial cable with extension of its inner conductor (6). When external RF thermal energy is delivered, the MRIHG can create a very localized and controlled heat spot, with the heating core at the junction of the inner conductor and outer conductor of the MRIHG (22). The RF power distribution is homogeneous within a distance of 0.5cm around the heating spot of the MRIHG (23). We placed the fiber optical temperature probe at the margin of the tumor to ensure the essential creation of RF heating within the tumor at a temperature of 42°C . In the current study, via serial *in vitro* and *in vivo* experiments, we have successfully validated the feasibility of combining the MRIHG-mediated heating at $40\text{--}42^{\circ}\text{C}$ with the application of gemcitabine, resulting in significant inhibition of the pancreatic tumor growth.

For the future application of this new approach, the advantages of using the MRIHG as a local heating source include: 1) the thin MRIHG can be easily positioned by any interventional device, via naturally existing lumens of the body (such as the biliary duct or vessels), closing to a target tumor area; 2) the MRIHG can be used as a multifunctional device, to simultaneously generate imaging and heating at the target area; 3) the MRIHG

technique may be combined with MR thermal mapping techniques to instantly monitor and control the location, distribution, and extent of the delivered therapeutic heat at the target tumor area during MR imaging (23).

It is known that diffusion magnetic resonance imaging can measure the mobility of water within tissues and, therefore, can serve as a surrogate bio-marker for both tissue cellularity and assessment of the treatment that occurs earlier than usual measures for assessing the tumor response (24). In the current study, a temporary decrease of ADC value occurred immediately in the animal group with RFH plus gemcitabine, at day 1 post-treatment. This phenomenon can be explained as a reflection of tumor intracellular edema induced by RFH (24, 25), demonstrating a prompt tumor response to the treatment. At days 7 and 14 after the treatment, the mean ADC value of the animal group with gemcitabine plus RFH increased and was significantly higher than those of other groups receiving different treatments. The ADC increase can be explained by more freedom for the water molecules due to overall cell loss, a reduction in cell density and an associated increase in the extracellular space (26). For the tumors in the RFH-only groups, the ADC is higher than that of pretreatment which correlates with the increased apoptosis index. The findings in ADC measurements represent the evidence that the change of ADC value is a sensitive biomarker of physiological response to hyperthermia-mediated chemotherapy of pancreatic cancers.

In conclusion, this study confirms that MRIHG-mediated localized RF heating can enhance the therapeutic effects of gemcitabine on pancreatic cancers, which can be efficiently monitored by DWI in-vivo. This study creates a potential groundwork for the efficient management of pancreatic malignancies using MR/RF-integrated local chemotherapy.

Acknowledgments

Founding support: This study was supported by an NIH RO1EBO12467 grant.

Abbreviations

RFH	Radiofrequency heat
MRIHG	MR-imaging-heating-guidewire
DMEM	Dulbecco's Modified Eagle Medium
PBS	Phosphate-buffered saline
T2WI	T2 weighted imaging
DWI	Diffusion-weighted imaging
RARE	Rapid acquisition with relaxation enhancement
ADC	Apparent diffusion coefficients
ROI	Region of interest
RTV	Relative tumor volume
TUNEL	Terminal deoxynucleotidyl transferase-mediated dUTP nick end labeling
AI	Apoptotic Index

References

1. Jemal A, Siegel R, Ward E, Hao Y, Xu J, Thun MJ. Cancer statistics, 2009. *CA: a cancer journal for clinicians*. 2009; 59(4):225–249. [PubMed: 19474385]

2. O'Reilly EM, Abou-Alfa GK. Cytotoxic therapy for advanced pancreatic adenocarcinoma. *Seminars in oncology*. 2007; 34(4):347–353. [PubMed: 17674963]
3. Burris H 3rd, Rocha-Lima C. New therapeutic directions for advanced pancreatic cancer: targeting the epidermal growth factor and vascular endothelial growth factor pathways. *The oncologist*. 2008; 13(3):289–298. [PubMed: 18378539]
4. Tschöep-Lechner KE, Milani V, Berger F, Dieterle N, Abdel-Rahman S, Salat C, Issels RD. Gemcitabine and cisplatin combined with regional hyperthermia as second-line treatment in patients with gemcitabine-refractory advanced pancreatic cancer. *International journal of hyperthermia*. 2013; 29(1):8–16. [PubMed: 23245336]
5. Partanen A, Yarmolenko PS, Viitala A, Appanaboyina S, Haemmerich D, Ranjan A, Jacobs G, Woods D, Enholm J, Wood BJ, Dreher MR. Mild hyperthermia with magnetic resonance-guided high-intensity focused ultrasound for applications in drug delivery. *International journal of hyperthermia*. 2012; 28(4):320–336. [PubMed: 22621734]
6. Du X, Qiu B, Zhan X, Kolmakova A, Gao F, Hofmann LV, Cheng L, Chatterjee S, Yang X. Radiofrequency-enhanced vascular gene transduction and expression for intravascular MR imaging-guided therapy: feasibility study in pigs. *Radiology*. 2005; 236(3):939–944. [PubMed: 16040894]
7. Manning HC, Merchant NB, Foutch AC, Virostko JM, Wyatt SK, Shah C, McKinley ET, Xie J, Mutic NJ, Washington MK, LaFleur B, Tantawy MN, Peterson TE, Ansari MS, Baldwin RM, Rothenberg ML, Bornhop DJ, Gore JC, Coffey RJ. Molecular imaging of therapeutic response to epidermal growth factor receptor blockade in colorectal cancer. *Clinical cancer research*. 2008; 14(22):7413–7422. [PubMed: 19010858]
8. Park SH, Moon WK, Cho N, Song IC, Chang JM, Park IA, Han W, Noh DY. Diffusion-weighted MR imaging: pretreatment prediction of response to neoadjuvant chemotherapy in patients with breast cancer. *Radiology*. 2010; 257(1):56–63. [PubMed: 20851939]
9. Ohno Y, Koyama H, Yoshikawa T, Matsumoto K, Aoyama N, Onishi Y, Sugimura K. Diffusion-weighted MRI versus 18F-FDG PET/CT: performance as predictors of tumor treatment response and patient survival in patients with non-small cell lung cancer receiving chemoradiotherapy. *AJR American journal of roentgenology*. 2012; 198(1):75–82. [PubMed: 22194481]
10. Kim H, Morgan DE, Buchsbaum DJ, Zeng H, Grizzle WE, Warram JM, Stockard CR, McNally LR, Long JW, Sellers JC, Forero A, Zinn KR. Early therapy evaluation of combined anti-death receptor 5 antibody and gemcitabine in orthotopic pancreatic tumor xenografts by diffusion-weighted magnetic resonance imaging. *Cancer research*. 2008; 68(20):8369–8376. [PubMed: 18922909]
11. Kyriazi S, Collins DJ, Messiou C, Pennert K, Davidson RL, Giles SL, Kaye SB, Desouza NM. Metastatic ovarian and primary peritoneal cancer: assessing chemotherapy response with diffusion-weighted MR imaging--value of histogram analysis of apparent diffusion coefficients. *Radiology*. 2011; 261(1):182–192. [PubMed: 21828186]
12. Yabuuchi H, Hatakenaka M, Takayama K, Matsuo Y, Sunami S, Kamitani T, Jinnouchi M, Sakai S, Nakanishi Y, Honda H. Non-small cell lung cancer: detection of early response to chemotherapy by using contrast-enhanced dynamic and diffusion-weighted MR imaging. *Radiology*. 2011; 261(2):598–604. [PubMed: 21852569]
13. Gołab J, Stokłosa T, Zagozdzon R, Kaca A, Giermasz A, Pojda Z, Machaj E, Dabrowska A, Feleszko W, Lasek W, Iwan-Osiecka A, Jakóbisziak M. G-CSF prevents the suppression of bone marrow hematopoiesis induced by IL-12 and augments its antitumor activity in a melanoma model in mice. *Annals of oncology*. 1998; 9(1):63–69. [PubMed: 9541685]
14. Chua YJ, Zalcborg JR. Pancreatic cancer--is the wall crumbling? *Annals of oncology : official journal of the European Society for Medical Oncology / ESMO*. 2008; 19(7):1224–1230. [PubMed: 18381371]
15. Herrmann R, Bodoky G, Ruhstaller T, Glimelius B, Bajetta E, Schüller J, Saletti P, Bauer J, Figer A, Pestalozzi B, Köhne CH, Mingrone W, Stemmer SM, Tàmas K, Kornek GV, Koeberle D, Cina S, Bernhard J, Dietrich D, Scheithauer W, Swiss Group for Clinical Cancer Research; Central European Cooperative Oncology Group. Gemcitabine plus capecitabine compared with gemcitabine alone in advanced pancreatic cancer: a randomized, multicenter, phase III trial of the Swiss Group for Clinical Cancer Research and the Central European Cooperative Oncology Group. *Journal of clinical oncology*. 2007; 25(16):2212–2217. [PubMed: 17538165]

16. Hildebrandt B, Hegewisch-Becker S, Kerner T, Nierhaus A, Bakhshandeh-Bath A, Janni W, Zumschlinge R, Sommer H, Riess H, Wust P, German Interdisciplinary Working Group on Hyperthermia. Current status of radiant whole-body hyperthermia at temperatures >41.5 degrees C and practical guidelines for the treatment of adults. The German 'Interdisciplinary Working Group on Hyperthermia'. *International journal of hyperthermia*. 2005; 21(2):169–183. [PubMed: 15764358]
17. Verwaal VJ, van Ruth S, de Bree E, van Sloothen GW, van Tinteren H, Boot H, Zoetmulder FA. Randomized trial of cytoreduction and hyperthermic intraperitoneal chemotherapy versus systemic chemotherapy and palliative surgery in patients with peritoneal carcinomatosis of colorectal cancer. *Journal of clinical oncology*. 2003; 21(20):3737–3743. [PubMed: 14551293]
18. Colombo R, Da Pozzo LF, Salonia A, Rigatti P, Leib Z, Baniel J, Calderera E, Pavone-Macaluso M. Multicentric study comparing intravesical chemotherapy alone and with local microwave hyperthermia for prophylaxis of recurrence of superficial transitional cell carcinoma. *Journal of clinical oncology*. 2003; 21(23):4270–4276. [PubMed: 14581436]
19. Ishikawa T, Kokura S, Sakamoto N, Ando T, Imamoto E, Hattori T, Oyamada H, Yoshinami N, Sakamoto M, Kitagawa K, Okumura Y, Yoshida N, Kamada K, Katada K, Uchiyama K, Handa O, Takagi T, Yasuda H, Sakagami J, Konishi H, Yagi N, Naito Y, Yoshikawa T. Phase II trial of combined regional hyperthermia and gemcitabine for locally advanced or metastatic pancreatic cancer. *International journal of hyperthermia*. 2012
20. Urano M, Kuroda M, Nishimura Y. For the clinical application of thermochemotherapy given at mild temperatures. *International journal of hyperthermia*. 1999; 15(2):79–107. [PubMed: 10323618]
21. Issels RD. Hyperthermia adds to chemotherapy. *Eur J Cancer*. 2008; 44(17):2546–2554. [PubMed: 18789678]
22. Qiu B, El-Sharkawy AM, Paliwal V, Karmarkar P, Gao F, Atalar E, Yang X. Simultaneous radiofrequency (RF) heating and magnetic resonance (MR) thermal mapping using an intravascular MR imaging/RF heating system. *Magnetic resonance in medicine*. 2005; 54(1):226–230. [PubMed: 15968681]
23. Qiu B, Yeung CJ, Du X, Atalar E, Yang X. Development of an intravascular heating source using an MR imaging guidewire. *Journal of magnetic resonance imaging : JMRI*. 2002; 16(6):716–720. [PubMed: 12451585]
24. Hamstra DA, Rehemtulla A, Ross BD. Diffusion magnetic resonance imaging: a biomarker for treatment response in oncology. *Journal of clinical oncology*. 2007; 25(26):4104–4109. [PubMed: 17827460]
25. Matsumoto Y, Kuroda M, Matsuya R, Kato H, Shibuya K, Oita M, Kawabe A, Matsuzaki H, Asaumi J, Murakami J, Katashima K, Ashida M, Sasaki T, Sei T, Kanazawa S, Mimura S, Oono S, Kitayama T, Tahara S, Inamura K. In vitro experimental study of the relationship between the apparent diffusion coefficient and changes in cellularity and cell morphology. *Oncology reports*. 2009; 22(3):641–648. [PubMed: 19639216]
26. Sala E, Kataoka MY, Priest AN, Gill AB, McLean MA, Joubert I, Graves MJ, Crawford RA, Jimenez-Linan M, Earl HM, Hodgkin C, Griffiths JR, Lomas DJ, Brenton JD. Advanced ovarian cancer: multiparametric MR imaging demonstrates response- and metastasis-specific effects. *Radiology*. 2012; 263(1):149–159. [PubMed: 22332064]

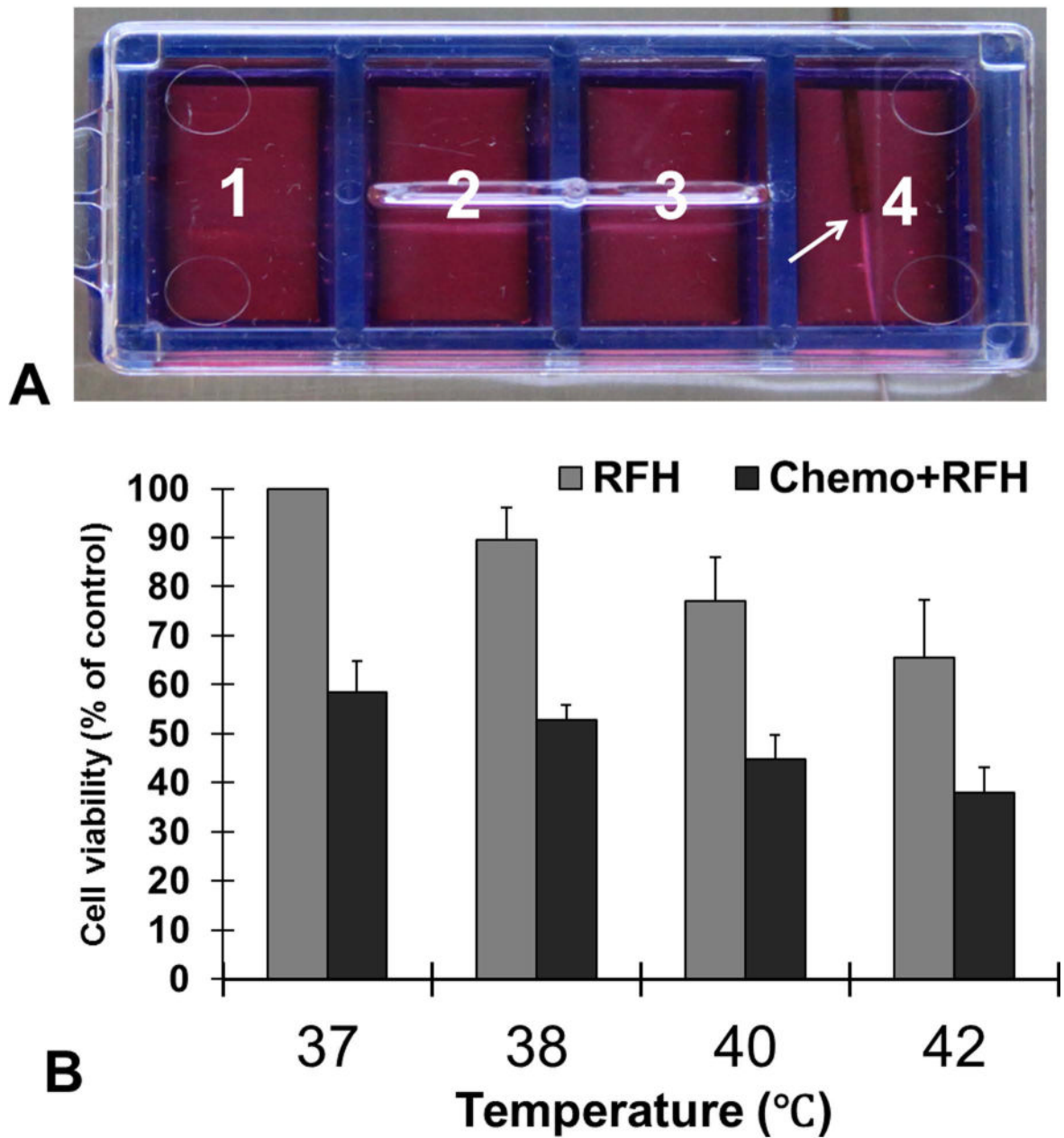


Fig. 1. (A) The in vitro experimental setup of RF heating (RFH) on cells. A 0.56-mm MR imaging-heating-guidewire (MRIHG) was positioned under the bottom of chamber 4, keeping the hotspot of the MRIHG at the center of chamber 4 (arrow). (B) Quantitative cells viability assay demonstrates that the relative cell viability is significantly decreased in chemotherapy +RFH group than in RFH-only and chemotherapy-only groups at all four temperature levels ($p < 0.05$).

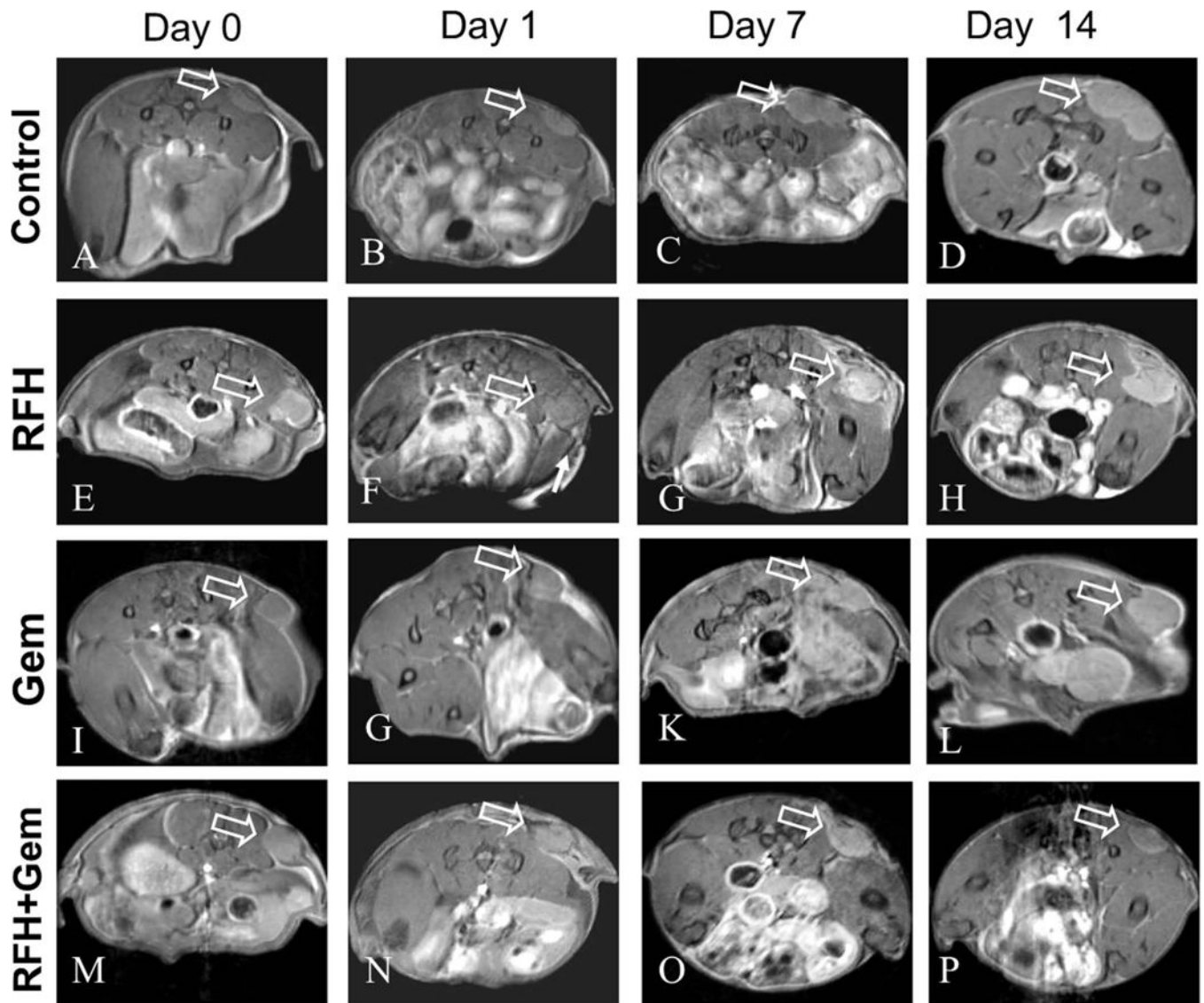


Fig. 2. Axial RARE T2-weighted images of mice pancreatic cancer xenografts in four groups receiving different treatments, showing homogeneous hyperintense tumor masses on the unilateral back of mice (arrows). Follow-up of tumor growths at different time points shows that, compared with the PBS (A-D), chemotherapy-only (I-L) and RFH-only (E-H) groups, the tumor size in the group treated by RFH-enhanced chemotherapy (M-P) was significantly decreased.

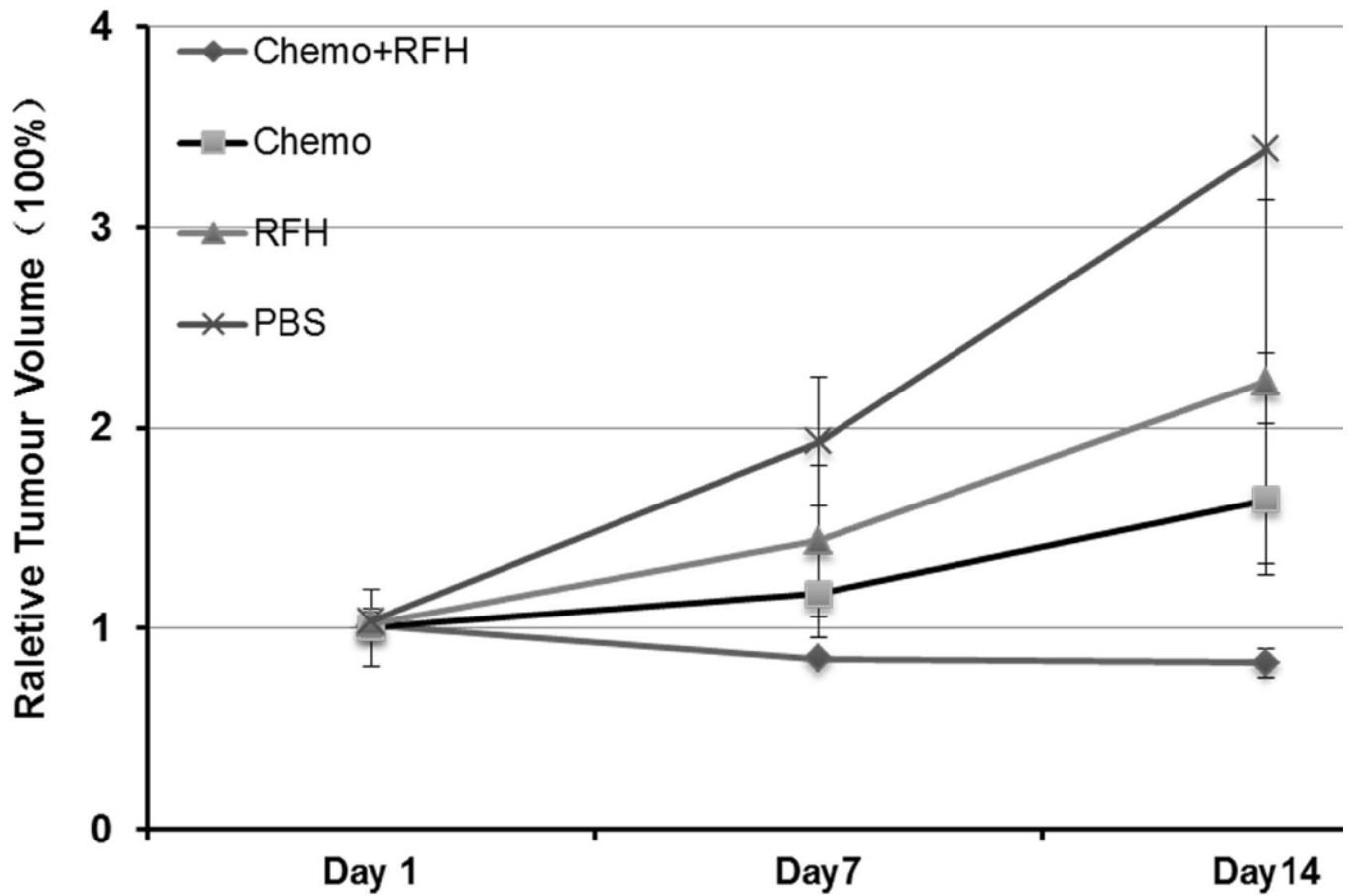


Fig. 3. Comparison of relative tumor volumes (RTV) between four groups receiving different treatments, shows that RFH-enhanced chemotherapy significantly inhibited the tumor growth with the lowest RTV at day 14 (0.82 ± 0.17) than chemotherapy-only (1.64 ± 0.44) and RFH- only (2.23 ± 0.90) groups ($P < 0.05$).

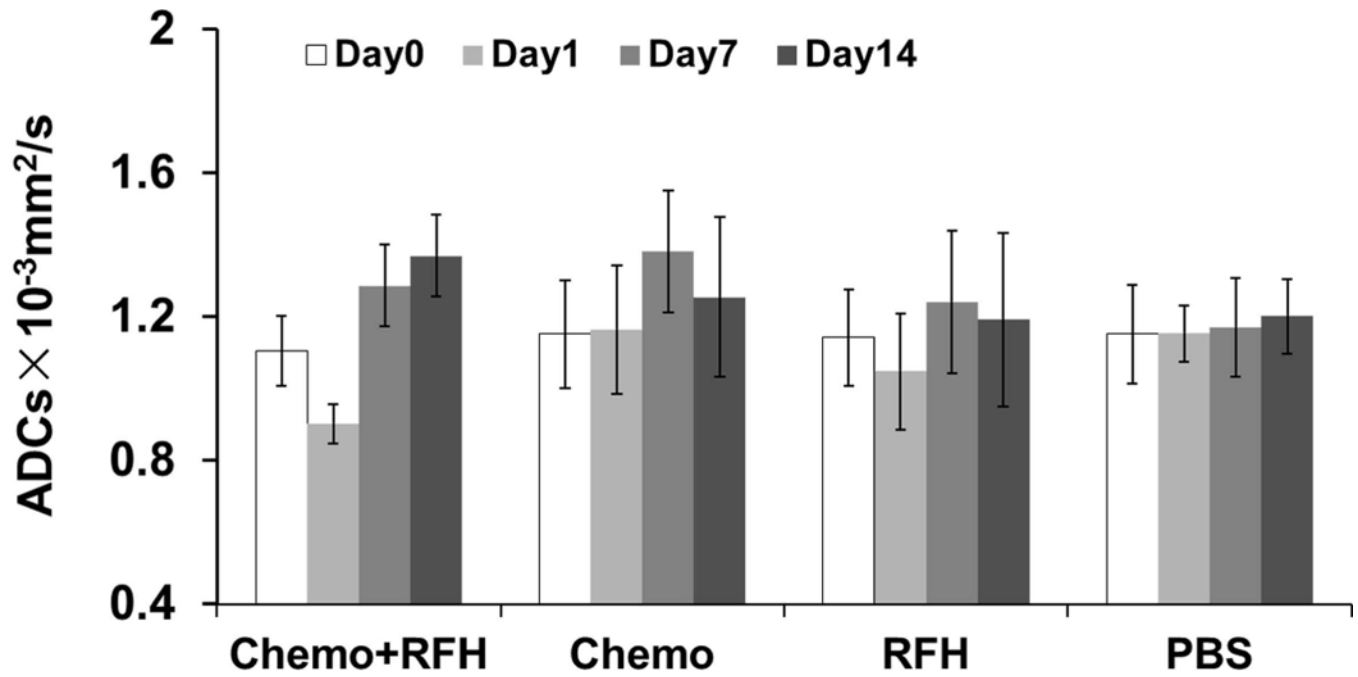


Fig. 4. ADCs of four animal groups with various treatments. The RFH-enhanced chemotherapy group demonstrated an immediate ADC decrease at day 1 and a following increase at day 7 and day 14, compared with the ADC at day 0 ($P=0.007, 0.01$ and 0.002). For the groups with chemotherapy-only, RFH-only and PBS (control), ADCs have no significant change.

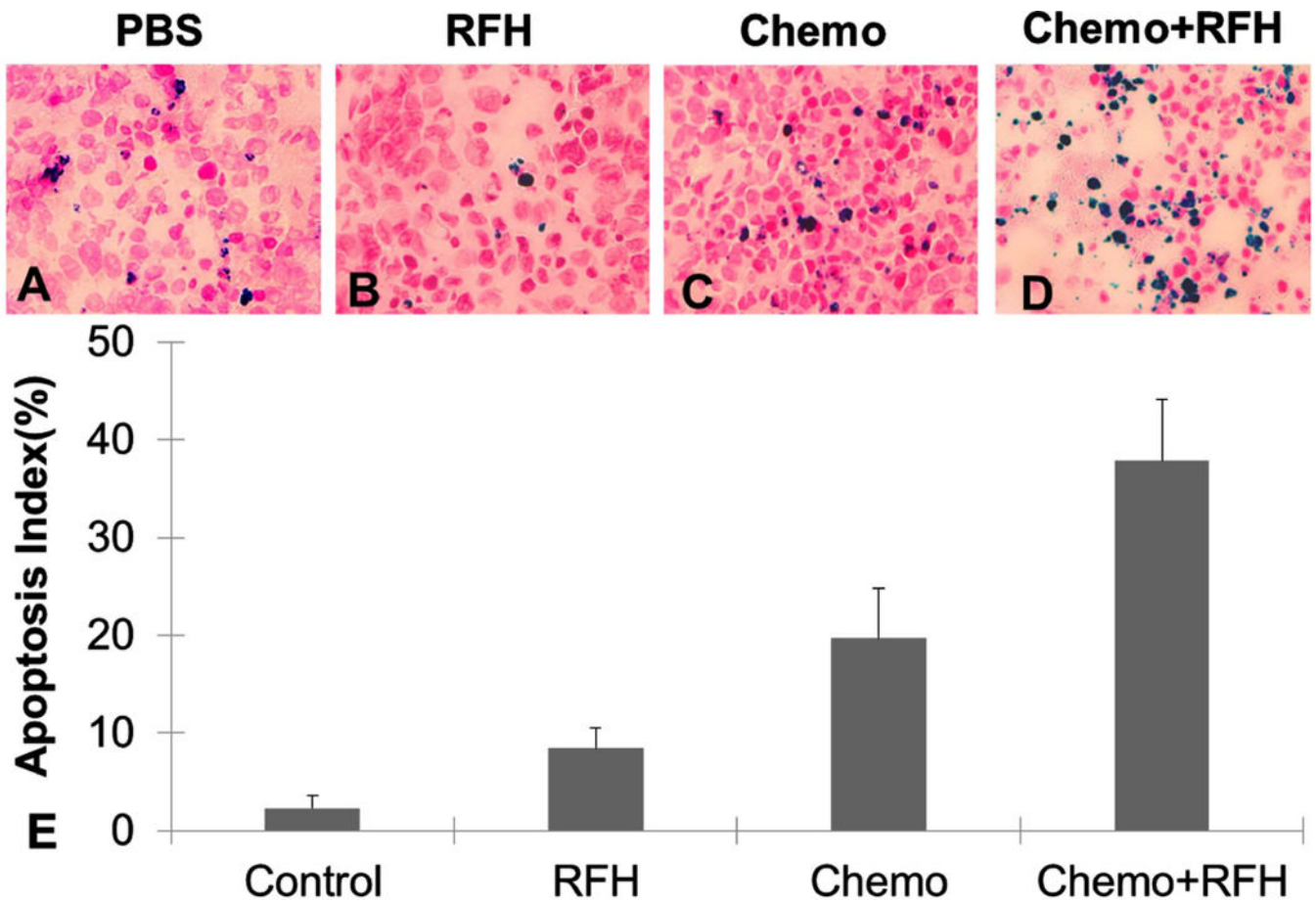


Fig. 5. Apoptosis analysis of tumors in four groups at day 14, demonstrates that more apoptotic cells (as blue spots in cells) in the cell group with chemotherapy + RFH (D) compared to those in other control groups with PBS (A), RFH-only (B), and chemotherapy-only (C). (E) Quantitative analysis of apoptosis shows the RFH-enhanced chemotherapy group has higher apoptotic index ($37\% \pm 6\%$) than PBS ($3\% \pm 1\%$), RFH-only ($8\% \pm 2\%$) and chemotherapy-only ($20\% \pm 5\%$) groups ($p < 0.05$).